CHARM AND CHARMONIUM IN THE QUARK-GLUON PLASMA

R. RAPP*, D. CABRERA and H. VAN HEES

Cyclotron Institute and Physics Department, Texas A&M University, College Station, Texas 77843-3366, U.S.A.
**E-mail: rapp@comp.tamu.edu*

In the first part of the talk, we briefly review the problem of parton-energy loss and thermalization at the Relativistic Heavy-Ion Collider and discuss how heavy quarks (charm and bottom) can help to resolve the existing experimental and theoretical puzzles. The second part of the talk is devoted to the properties of heavy quarkonia in the (strongly interacting) Quark-Gluon Plasma (sQGP) and their consequences for observables in heavy-ion collisions.

Keywords: Quark-Gluon Plasma, Heavy Quarks and Quarkonia, Ultrarelativistic Heavy-Ion Collisions

1. Introduction

Experiments at the Relativistic Heavy-Ion Collider (RHIC) suggest that the matter created in semi-/central Au-Au collisions at $\sqrt{s_{NN}}$=200 GeV constitutes an equilibrated, strongly interacting medium at high energy density, well above the critical one at the expected phase boundary, $\epsilon_c \simeq 1\,\mathrm{GeV/fm^3}$ (cf. the experimental assessment papers[1,2] and references therein). This conclusion is essentially based on three evidences: (i) at low transverse momenta, $p_T \leq$2-3 GeV (comprising $\sim$99% of the produced hadrons), ideal relativistic hydrodynamics describes well the single-particle spectra and their azimuthal asymmetry, $v_2(p_T)$; the underlying collective expansion follows from kinetic equilibration times of around $\tau_0 \simeq 0.5\,\mathrm{fm}/c$, implying rapid (local) thermalization of the system at initial energy densities of about $\epsilon_0 \simeq 30\,\mathrm{GeV/fm^3}$. (ii) at high momenta, $p_T \geq$5-6 GeV, the production of hadrons is suppressed by a factor of 4-5 relative to elementary p-p (or d-Au) collisions. This has been interpreted as energy loss of energetic partons traveling through an almost opaque high gluon-density medium. (iii) at intermediate momenta, $p_T \simeq$2-6 GeV, surprisingly large baryon-to-meson

ratios, as well as an empirical scaling of the hadron v_2 according to its constituent quark content, has been interpreted as quark coalescence as the prevalent hadronization mechanism in this regime, and thus as partonic degrees of freedom being active. The microscopic mechanisms underlying thermalization and energy loss, however, are not well understood yet. In fact, the jet quenching of light partons is so strong that high-p_T particle emission appears to be mostly limited to the surface of the fireball, rendering a precise determination of the corresponding transport coefficient (and maximal energy density) difficult. While earlier approaches assumed the dominance of radiative energy loss via medium-induced gluon radiation (which prevails in the limit of high jet energies) cf. [3], it has been realized subsequently that elastic ($2\leftrightarrow2$) scattering processes cannot be neglected at currently accessible $p_T\leq$10-15 GeV at RHIC. Moreover, none of the evidences (i)-(iii) is directly connected to the fundamental properties distinguishing the Quark-Gluon Plasma (QGP) from hadronic matter, namely the deconfinement of color charges and the restoration of the spontaneously broken chiral symmetry (which is believed to generate most of the visible mass in the universe).

Heavy-quark (HQ) observables are expected to provide new insights into the aforementioned problems (with the exception of chiral symmetry restoration). On the one hand, charm (c) and bottom (b) quarks, due to their relatively large mass, should suffer less energy loss and undergo delayed thermalization when traversing the QGP, and thus be more sensitive to the interactions with thermal partons than light quarks and gluons. Therefore, it came as a surprise when the measurement of single-electron ($e^{\pm}$) spectra associated with the semileptonic decay of open-charm (and -bottom) hadrons showed a factor 4-5 suppression[4,5], very comparable to what has been found for pions. In addition, the observed values for the $e^{\pm}$ elliptic flow, $v_2^e(p_T)$, reach up to 10% at $p_T\simeq$2 GeV, indicating the build-up of substantial *early* collectivity of c quarks. These observations reinforced the implementation of elastic energy-loss processes into the theoretical description of the spectra[6–10]. On the other hand, HQ bound states (quarkonia), due to their small size/large binding, are suitable probes of a surrounding medium of sufficiently high density. E.g., for a typical (ground-state) charmonium of size r=0.25 fm, the relevant parton density at which significant modifications are to be expected is $n\approx3/(4\pi r^3)\approx$10-20 fm^{-3}, which for an ideal QGP (with N_f=2.5 massless flavors) translates into a temperature of $T\approx$270 MeV$\approx1.5T_c$. Indeed, recent lattice QCD (lQCD) calculations indicate that J/ψ and η_c states survive in a QGP up to $\sim2T_c$. The theoretical

challenge is then to disentangle and quantify (a) medium modifications of the binding potential (e.g., color screening), (b) parton-induced dissociation reactions, and (c) in-medium changes of the HQ mass which affects both the bound-state mass and its decay threshold, as well as to identify and establish connections to observables in heavy-ion collisions.

In the first part of the talk (Sec. 2), we evaluate HQ diffusion and thermalization in the QGP employing both perturbative and *nonperturbative* elastic interactions. This problem is particularly suited to a Fokker-Planck approach for Brownian motion in a thermal background[11], which allows to describe both the quasi-thermal and kinetic regime, and its transition. A Langevin simulation for c and b quarks in an expanding QGP at RHIC is supplemented with coalescence (and fragmentation) at T_c, thus implementing all of the three main features (i)-(iii) of the initial RHIC data. In the second part of the talk (Sec. 3), we discuss in-medium properties of heavy quarkonia, including information from lQCD. We outline a T-matrix approach in which HQ potentials from lQCD are used as input to simultaneously describe bound and scattering states. This enables a comprehensive evaluation of euclidean correlation functions, which in turn can be checked against rather accurate results from lQCD. We briefly discuss how in-medium quarkonium properties reflect themselves in observables in ultrarelativistic heavy-ion collisions. Sec. 4 contains our conclusions.

2. Open Charm and Bottom in the QGP

Recent calculations of hadronic spectral functions in a QGP, both within lQCD and lQCD-based potential models, suggest that resonance (or bound) states persist up to $2T_c$, for both heavy- ($Q\bar{Q}$) and light-quark ($q\bar{q}$) systems. We conjectured[6] that this also holds for heavy-light systems, and therefore could lead to significantly faster thermalization for c and b quarks as compared to perturbative QCD (pQCD) processes. Even at T=350 MeV (which roughly corresponds to initial temperatures at RHIC) and for α_s=0.4, elastic pQCD scattering, which is dominated by t-channel gluon exchange, results in a thermal relaxation time for c quarks above 10 fm/c, well above a the typical QGP lifetime of $\tau_{\rm QGP}\sim$5 fm/c. Recent data on single-electron spectra associated with semileptonic heavy-meson decays have corroborated the need for nonperturbative HQ interactions in the QGP. As shown in Fig. 1, perturbative energy-loss calculations appear insufficient to describe the strong suppression in the p_T-spectra (left panel, using both elastic and radiative interactions) and the large $v_2(p_T)$ (right panel, using radiative energy loss with a substantially upscaled transport coefficient). While the

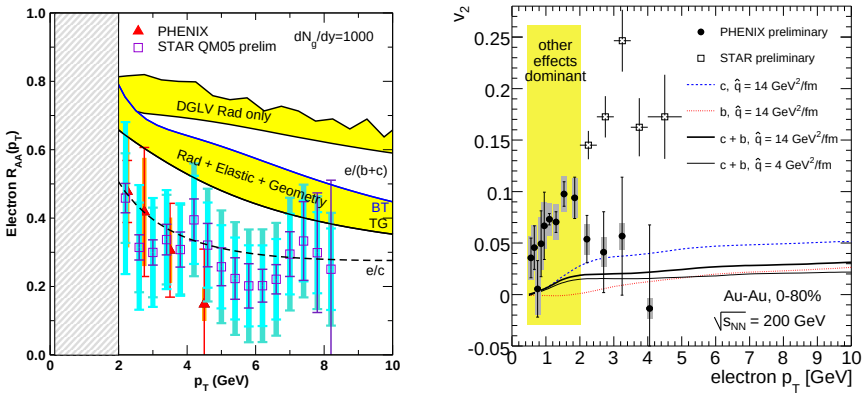

Fig. 1. Perturbative QCD energy-loss calculations for $e^{\pm}$ spectra from semileptonic heavy-meson decays. Left panel: nuclear suppression factor[10], right panel: elliptic flow[12].

plots indicate a (lower) applicability limit of the pQCD energy-loss approach of $p_T^e \simeq 2\,\mathrm{GeV}$, we will argue below that nonperturbative effects may be relevant (or even dominant) up to at least $p_T^e \simeq 5\,\mathrm{GeV}$. In particular, radiative energy-loss calculations typically do not include the backward reactions (detailed balance) which are essential for building up collective behavior of the heavy quarks in the expanding thermal medium. As mentioned above, in this context a Brownian-motion approach is well suited to address the thermalization of the heavy quarks[6,7,11,13]. Upon expanding the Boltzmann equation in small momentum transfers, one arrives at a Fokker-Planck equation for the HQ distribution function, f,

$$\frac{\partial f}{\partial t} = \gamma \frac{\partial (pf)}{\partial p} + D_p \frac{\partial^2 f}{\partial p^2} \ , \tag{1}$$

with (momentum) drag (γ) and diffusion (D_p) constants (related via $T = D_p/\gamma M_Q$). The latter are calculated from corresponding matrix elements for HQ scattering off light partons. As mentioned above, our main ingredient here are resonance-mediated elastic interactions in s- and u-channel (cf. left panel of Fig. 2) which we model with an effective Lagrangian according to[6]

$$\mathcal{L} = -G\ \bar{Q}\ \Gamma\ \frac{1+\not{v}}{2}\ \Phi\ q + \mathrm{h.c}\ ; \tag{2}$$

Φ is the resonance field representing "D" and "B" mesons, which we dress by evaluating the corresponding one-loop (Q-$\bar{q}$) selfenergy. Parameters of the model are the resonance mass (which we fix at 0.5 GeV above the Q-$\bar{q}$ threshold) and coupling constant, G, which determines the resonance width. HQ and chiral symmetry (above T_c) imply degeneracy of the pseudo-/scalar

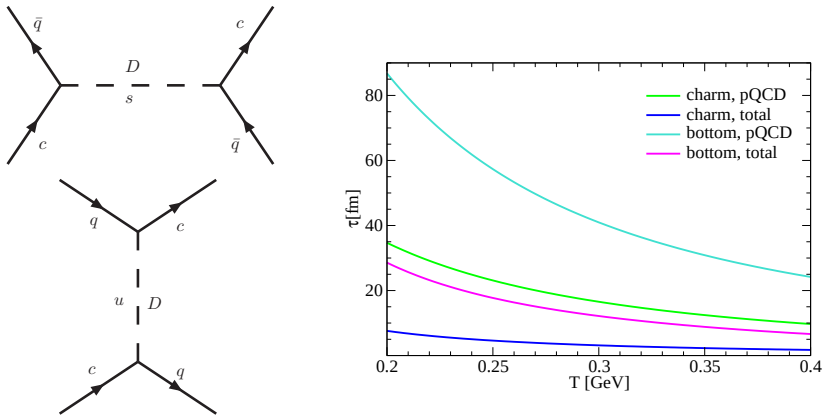

Fig. 2. Elastic HQ-scattering processes via D-(B-)meson like resonances (left panel) and resulting thermalization times compared to pQCD results (right panel)[6].

and axial-/vector channels represented by the Dirac matrices, Γ. The temperature dependence of the resulting thermal relaxation times, $\tau_Q = \gamma^{-1}$, for c- and b-quarks shows a factor of $\sim$3 reduction compared to calculations where only pQCD elastic scattering is accounted for (right panel of Fig. 2). This is very significant for c-quarks as τ_c is now comparable to (or even below) the duration of the QGP phase at RHIC ($\tau_{\rm QGP}\sim 5\,{\rm fm}/c$), whereas $\tau_b > \tau_{\rm QGP}$ still, due to the large b-quark mass.

The T- and p-dependent drag and diffusion coefficients have been implemented into a relativistic Langevin simulation[6] using an (elliptic) thermal fireball expansion for (semi-) central Au-Au collisions at RHIC as a background medium, where the bulk flow is adjusted to hydrodynamic simulations in accordance with experiment. At the end of the QGP phase (which terminates in a mixed phase at T_c=180 MeV), the c- and b-quark output distributions from the Langevin simulation are subjected to hadronization into D- and B-mesons using the quark-coalescence model of Ref. [14]. Since the probability for coalescence is proportional to the light-quark distribution functions, it preferentially occurs at lower p_T; "left-over" heavy quarks are hadronized via δ-function fragmentation. The extra contribution to momentum and v_2 from the light quarks *increases both* the $R_{AA}(p_T)$ and $v_2(p_T)$ of the heavy-meson spectra, relative to a scheme with fragmentation only. Rescattering in the hadronic phase has been neglected. The resulting D- and B-meson spectra are decayed semileptonically resulting in a nuclear suppression factor and elliptic flow which compare reasonably well with recent RHIC data[4,5,15] up to $p_T \simeq 5\,{\rm GeV}$ (Fig. 3). At higher momenta, radiative

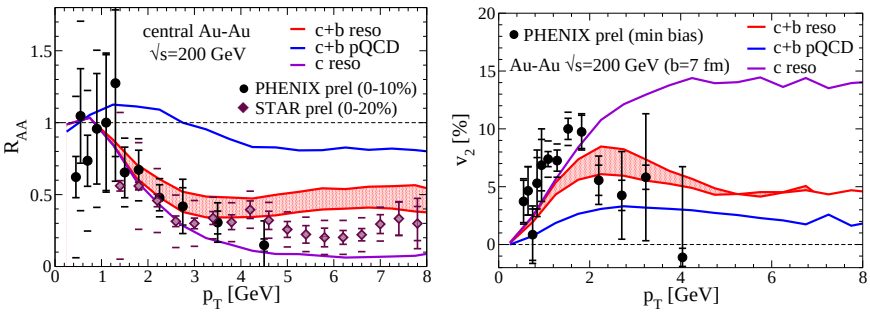

Fig. 3. Calculations for single-electron spectra arising from semileptonic heavy-meson decays. Left panel: Nuclear suppression factor right panel: elliptic flow.

energy loss (not included here) is expected to contribute significantly[a].

Another issue in interpreting the semileptonic $e^{\pm}$ spectra concerns the relative contributions of charm and bottom. Since bottom quarks are much less affected by rescattering effects, their contribution reduces the effects in both R_{AA} and v_2 appreciably. Following Refs. [9,17], we have determined the initial charm spectra by reproducing D- and D^*-spectra in d-Au collisions[18], calculated the pertinent $e^{\pm}$ spectra and assigned the missing yield relative to the data[19] to bottom contributions. In this way, the crossing between charm and bottom contribution in p-p collisions occurs at $p_T \simeq 5\,\mathrm{GeV}$. Due to the strong quenching of the c-quark spectra in the QGP this crossing is shifted down to $p_T \simeq 2.5\text{-}3\,\mathrm{GeV}$ in Au-Au collisions. For charm contributions only, our nonperturbative rescattering mechanism results in a pertinent electron R_{AA} as low as 0.1 and an elliptic flow as large as 14%. Thus, the severeness of the "$e^{\pm}$ puzzle" partially hinges on the baseline spectra in more elementary systems (p-p and d-Au). Obviously, a direct measurement of D-mesons in Au-Au would be very valuable.

3. Heavy Quarkonia in the QGP

3.1. *Potential Models, Spectral Functions and Lattice QCD*

Heavy quarkonia (c-$\bar{c}$ and b-$\bar{b}$ bound states) have long been identified as suitable objects to quantitatively investigate the properties of QCD, including color confinement[20]. A particularly appealing feature is the applicability

[a]Note that in a chemically equilibrated QGP, the effects of induced gluon radiation are presumably smaller than in a pure gluon plasma as assumed in Refs. [10,12]; an estimate of (some) 3-body scattering diagrams has been performed in Ref. [16].

of potential models as a nonrelativistic effective-theory approximation to QCD (cf. Ref. [21] for a recent review). In the vacuum, the heavy-quarkonium spectrum is indeed reasonably well described by the "Cornell potential", consisting of a Coulomb plus linear confining term. Subsequently it was realized that, when immersing quarkonia into a medium of deconfined color charges, Debye screening will reduce the binding and eventually lead to the dissolution of the bound state[22,23]; already slightly above T_c, a substantial (factor ∼2-3) reduction in charmonium and bottomonium binding energies, ε_B, has been found, together with the possibility that the (S-wave) ground states ($\eta_{c,b}$, J/ψ, $\Upsilon(1S)$) survive (well) above T_c. Modern lQCD (-based) calculations qualitatively support this picture: On the one hand, directly extracted charmonium spectral functions (in quenched approximation) indicate resonance peaks up to $\sim 2T_c$[24,25]. On the other hand, (both quenched and unquenched) lQCD results for the (color-singlet) free energy,

$$F_{Q\bar{Q}}(r;T) = U_{Q\bar{Q}}(r;T) - TS_{Q\bar{Q}}(r;T) \ , \tag{3}$$

have been implemented into potential models within a Schrödinger[26–29] or Lippmann-Schwinger equation[30]. There is an ongoing debate as to which quantity ($F_{Q\bar{Q}}$, the internal energy $U_{Q\bar{Q}}$, or a linear combination thereof[31]) is the most appropriate one to use as a potential. Maximal binding is obtained with $U_{Q\bar{Q}}$, and even in this case, the ground-state charmonium (bottomonium) binding energies are reduced to $\varepsilon_B \simeq$0.1-0.2 GeV (0.3-0.6 GeV) at $T \simeq 1.5\ T_c$, compared to ∼0.6 GeV (1.1 GeV) in vacuum. However, a quantitative description of in-medium modifications of quarkonia requires at least two additional components, i.e., the effects of parton-induced dissociation reactions and of in-medium HQ masses. The objective is thus to construct an approach that (i) is consistent with finite-T lQCD and (ii) allows for reliable applications to observables in heavy-ion collisions. Only then the original idea[22] of using quarkonia as a tool to identify (and characterize) confinement (or at least color screening) may be realized.

The interplay of medium effects becomes more transparent in terms of the charmonium propagator, schematically written as (nonrelativistic)[b]

$$D_\Psi(\omega;T) = \left[\omega - (2m_c^* - \varepsilon_B) + \mathrm{i}\Gamma_\Psi\right]^{-1} \ . \tag{4}$$

It shows that screening (affecting the binding energy and thus the real part of the inverse propagator), and parton-induced dissociation (governing the

[b]Writing Eq. (4) in this form implies that the Q-$\bar{Q}$ potential is strong enough to generate a pole in the scattering amplitude. A microscopic (T-matrix) approach is discussed below.

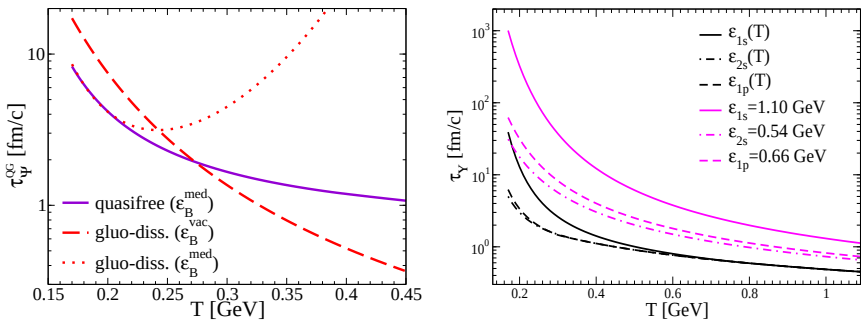

Fig. 4. Lifetimes of J/ψ (left panel, gluo-dissociation vs. quasifree dissociation mechanisms[34]) and Y states (right panel, quasifree dissociation[35]) in the QGP.

width, Γ_Ψ, of the spectral function, Im D_Ψ) are not mutually exclusive but have to be taken into account simultaneously[32].

The inelastic width (or dissociation rate) can be expressed as

$$\Gamma_\Psi = (\tau_\Psi)^{-1} = \int \frac{d^3k}{(2\pi)^3}\; f^p(\omega_k, T)\; v_{\rm rel}\; \sigma_\Psi^{\rm diss}(s) \qquad (5)$$

in terms of (thermal) parton-distribution functions, f^p (p=$q, \bar{q}, g$), and the parton-induced break-up cross section, $\sigma_\Psi^{\rm diss}$. The latter has first been evaluated for gluo-dissociation[33], $g + \Psi \to c + \bar{c}$, using Coulomb wave-functions for the quarkonia, leading to a T-dependent J/ψ lifetime as shown in the left panel of Fig. 4. For the vacuum J/ψ binding energy, ε_B=0.63 GeV, the lifetime is well behaved showing a rather steep decrease with T (dashed line). However, if an in-medium binding energy is used as following from screened (or lQCD) potentials, the lifetime is initially reduced (dotted line), but if the binding energy drops below ∼0.1 GeV, the phase space in the gluo-dissociation reaction strongly shrinks leading to an unphysical increase of the J/ψ lifetime with T. This artifact is even more pronounced for the less bound excited states (χ_c, ψ'). This problem has been remedied by introducing the "quasifree" dissociation process[34], $p + \Psi \to p + c + \bar{c}$, where a parton knocks out the Q (or $\bar{Q}$) from the bound state. With reasonable values for the strong coupling constant ($\alpha_s \simeq 0.25$) the resulting charmonium widths are in the ∼0.1 GeV range for $T \sim 1.5\ T_c$ (as relevant for RHIC) with a well-behaved T-dependence. The order of magnitude of the inelastic width is easily reproduced using a simplified estimate of Eq. (5) according to $\Gamma_\Psi \approx n_p(T)\sigma_{\rm diss} v_{\rm rel}$; with a parton density $n_p \simeq 10\,{\rm fm}^{-3}$ (at $T \approx 0.25$ GeV), a cross section of 1 mb and $v_{\rm rel}$=1/2 one finds $\Gamma_\Psi \approx 0.1$ GeV.

When applied to bottomonia, the same arguments apply[35]; the right

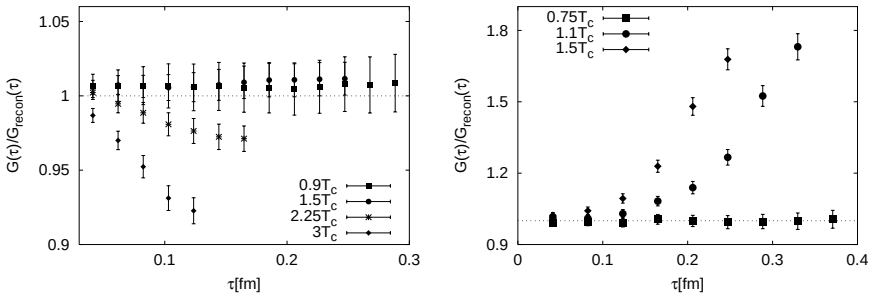

Fig. 5. Finite-temperature euclidean correlation functions computed in lQCD in the pseudoscalar (η_c, left panel) and scalar (χ_c, right panel) channels[25].

panel of Fig. 4 illustrates the impact of in-medium binding energies on bottomonium dissociation: in the RHIC temperature regime, screening may lead to up to a factor of ∼20 (!) reduction in the ground-state $\Upsilon(1S)$ lifetime, bringing it down to ∼2-5 fm/c at T=0.3-0.4 GeV. This has important consequences for bottomonium suppression at RHIC (as elaborated in Sec. 3.2 below), rendering it a sensitive probe of color screening[35].

A key issue for model descriptions of quarkonium spectral functions in the QGP is the implementation of constraints from lQCD. The standard object computed on the lattice is (the thermal expectation value of) a hadronic current-current correlation function in euclidean time, τ (and at zero 3-momentum), in quantum-number channel, α[36],

$$G_\alpha(\tau;T) = \langle j_\alpha(\tau) j_\alpha^\dagger(0)\rangle \ . \tag{6}$$

The connection to the spectral function, σ_α, is given by a convolution with a temperature kernel as

$$G_\alpha(\tau;T) = \int_0^\infty d\omega \ \sigma_\alpha(\omega;T) \ \frac{\cosh[\omega(\tau-1/2T)]}{\sinh[\omega/2T]} \ . \tag{7}$$

While euclidean correlators can be computed with good accuracy (Fig. 5), their limited temporal extent at finite T, $0\leq\tau\leq 1/T$, renders the extraction of (Minkowski) spectral functions more difficult. On the contrary, model calculations of spectral functions are readily integrated via Eq. (7) and compared to the rather precise euclidean correlators from lQCD[37,29]. To better exhibit the T-dependence induced by the spectral function, both lattice and model results for $G_\alpha(\tau;T)$ are commonly normalized to the so-called "reconstructed" correlator, which follows from Eq. (7) by inserting a free spectral function, $\sigma_\alpha(\omega, T=0)$.

Eq. (6) requires the knowledge of the quarkonium spectral function at all (positive) energies. A schematic decomposition consists of a bound-state part and a continuum,

$$\sigma_\alpha(\omega) = \sum_i 2M_i F_i^2 \delta(\omega^2 - M_i^2) + \frac{3}{8\pi^2}\,\omega^2\, f_{\rm cont}(\omega, E_{\rm thr})\Theta(\omega - E_{\rm thr}) \ , \quad (8)$$

where, for fixed α, i runs over all bound states with masses M_i and couplings F_i, and the threshold energy ($E_{\rm thr}$) and function $f_{\rm cont}$ characterize the onset and plateau of the continuum (usually taken from pQCD).

In Ref. [29], T-dependent bound-state masses and couplings have been evaluated by solving a Schrödinger equation with in-medium potentials (screened Cornell or lQCD internal energy, $U_{Q\bar{Q}}$); the threshold energy has been inferred from the asymptotic ($r \to \infty$) value of the respective potential, $E_{\rm thr}^{\rm med}(T) = 2m_c + V(r \to \infty; T)$ (which monotonously decreases for $T > T_c$). For the scalar (χ_c) channel it has been found that, despite a rather quickly dissolving bound-state contribution, the correlator increases significantly (consistent with the lattice result in Fig. 5, right panel), due to the decreasing continuum threshold. The latter also leads to an increasing pseudoscalar correlator, which is not favored by lQCD (Fig. 5, left panel).

In Ref. [38] the separation of bound-state and continuum parts is improved by employing a T-matrix approach[39,30] for the Q-$\bar{Q}$ interaction,

$$T_\alpha(E; q', q) = V_\alpha(q', q) - \frac{2}{\pi}\int_0^\infty dk\, k^2\, V_\alpha(q', k)\, G_{\bar{Q}Q}(E; k)\, T_\alpha(E; k, q) \ . \quad (9)$$

For V_α the Fourier transformed and partial-wave expanded lQCD internal energy has been used. Spin-spin (hyperfine) interactions are neglected implying degeneracy of states with fixed angular momentum (S-wave: η_c and J/ψ, P-wave: $\chi_{c0,1,2}$). $G_{\bar{Q}Q}(E; k)$ denotes the intermediate 2-particle propagator including quark selfenergies. The correlation and spectral functions follow from closing the external legs with 3-momentum integrations as

$$G_\alpha(E) = \int G_{\bar{Q}Q} + \int G_{\bar{Q}Q} \int T_\alpha\, G_{\bar{Q}Q} \ , \ \sigma_\alpha(E) = a\ {\rm Im}G_\alpha(E) \ , \quad (10)$$

where the coefficient a depends on the channel α. For a fixed c-quark mass of m_c=1.7 GeV, the resulting charmonium spectral functions confirm that bound states are supported in the S-wave up to $\sim 3T_c$ while dissolved in the P-wave below 1.5 T_c, see Fig. 6. In both cases, however, one finds a large (nonperturbative) enhancement of strength in the threshold region. The corresponding euclidean correlators are displayed in Fig. 7, normalized to a reconstructed one using the vacuum bound-state spectrum and a perturbative continuum with onset at the free $D\bar{D}$ threshold, $E_{\rm thr}^{\rm vac}$=$2m_D \simeq$3.75 GeV.

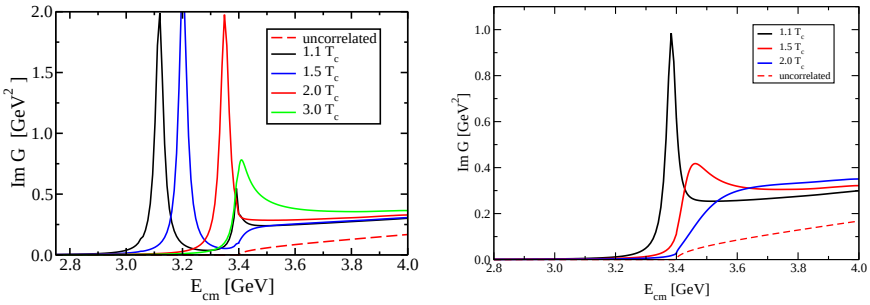

Fig. 6. S- (left panel) and P-wave (right panel) charmonium-spectral functions from the T-matrix approach with an lQCD-internal energy as potential[38].

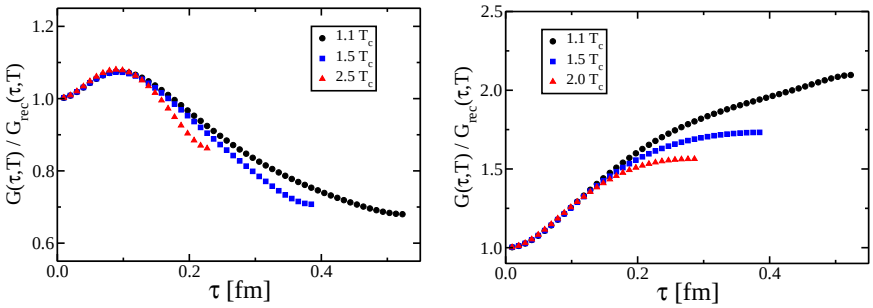

Fig. 7. Normalized euclidean correlation function for S- (left panel) and P-wave (right panel) charmonium states within a T-matrix approach using lQCD-internal energies[38].

The χ_c correlator (right panel) is well above one, both due to a lower in-medium threshold, $E_{\rm thr}^{\rm med}$=$2m_c$=3.4 GeV, and the nonperturbative rescattering enhancement. While this is qualitatively consistent with lQCD, the temperature dependence is opposite, indicative for a further threshold decrease with temperature. In the η_c channel (left panel), the significant reduction in binding energy (due to color screening) reduces the correlator at large τ, qualitatively in line with lQCD. In fact, the latter shows less reduction, leaving room for a T-dependent reduction of $E_{\rm thr}^{\rm med}$ as well.

The scattering equation (9) is furthermore well suited to study finite-width effects. E.g., when dressing the c-quarks with an imaginary self-energy corresponding to Γ_c=50 MeV, inducing a charmonium width of $\Gamma_\Psi \simeq$100 MeV (as in the left panel of Fig. 4), the euclidean correlators vary by no more than 2%. This indicates that there is rather little sensitivity to phenomenologically relevant values for the quarkonium widths.

3.2. *Quarkonium Phenomenology in Heavy-Ion Collisions*

The formation of thermalized matter above T_c in ultrarelativistic heavy-ion collisions (recall the discussion in the introduction) provides the basis for describing the production systematics of quarkonia in terms of their in-medium properties as discussed in the previous section. The suppression factor for the initially produced number of quarkonia may be schematically written as proceeding through 3 stages,

$$S_{\rm tot} = \exp(-\sigma_{\rm nuc}^{\rm abs}\ \varrho_N\ L)\ \exp(-\Gamma_{\rm QGP}\ \tau_{\rm QGP})\ \exp(-\Gamma_{\rm HG}\ \tau_{\rm HG}). \qquad (11)$$

With the suppression in the hadron gas (HG) believed to be small, and the ("pre-equilibrium") nuclear absorption (cross section) inferred from p-A experiments, the suppression factor directly probes the dissociation rate of Ψ's in the QGP. The observed J/ψ-suppression pattern at SPS can indeed be well described using the quasifree dissociation process with in-medium binding energies consistent with lQCD-potential models[34,40].

At RHIC energy, copious production of $c\bar{c}$ pairs ($N_{c\bar{c}}\simeq$20 in central $\sqrt{s}$=200 AGeV Au-Au[41], compared to 0.2 at SPS) opens the possibility of secondary charmonium production[42,34]. This is, after all, required by detailed balance in the dissociation reaction, $\Psi+g \rightleftharpoons c+\bar{c}+X$, provided the Ψ state still exists at the given temperature[40,43]. If, in addition, the c-quarks are close to thermal equilibrium, one can apply the rate equation,

$$\frac{dN_\Psi}{dt} = -\Gamma_\Psi[N_\Psi - N_\Psi^{\rm eq}(T)] \quad , \qquad (12)$$

for the time evolution of the J/ψ number. Pertinent predictions (upper solid line in the left panel of Fig. 8) agree reasonably well with current PHENIX data[44] suggesting that the regeneration component becomes substantial in central Au-Au. Corrections due to incomplete c-quark thermalization, as well as a lower dissociation (and thus formation) temperature, reduce the regeneration (lower solid curves in the left panel of Fig. 8). It has also been suggested[45] that available J/ψ data at SPS and RHIC are compatible with suppression of only χ_c and ψ' (which make up $\sim$40% of the inclusive J/ψ yield in p-p), with the direct J/ψ's being unaffected. However, if at RHIC the J/ψ width is of order 0.1 GeV (cf. previous section) and the QGP lifetime at least 2 fm/c, one finds a QGP suppression factor of $S_{\rm QGP}\simeq$0.4.

Finally, turning to Υ production, the increase of the Υ dissociation rate due to color screening (recall right panel of Fig. 4) could lead to a Υ yield in central Au-Au (right panel of Fig. 8) which is more suppressed for the J/ψ (left panel), and thus provide a rather striking QGP signature[35].

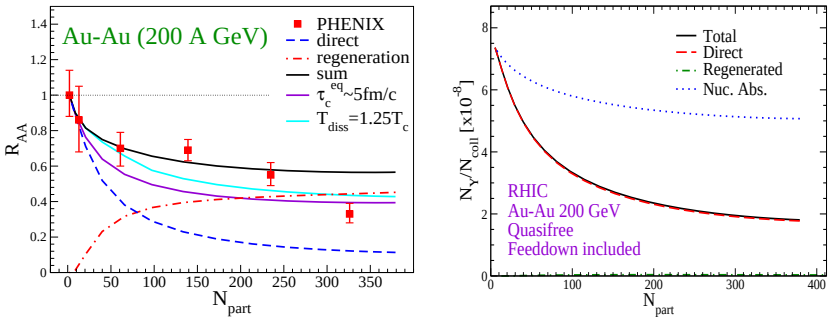

Fig. 8. Centrality dependence of the nuclear modification factor for J/ψ (left panel)[40,46] and Υ (right panel)[35] at RHIC.

4. Conclusions

Charm and bottom hadrons are valuable sensors of the sQGP. In the open-flavor sector, the inadequacy of pQCD to account for the suppression and collectivity of current $e^{\pm}$ spectra at RHIC may be a rather direct indication of nonperturbative rescattering processes above T_c. We have elaborated these in a concrete example using (elastic) resonance interactions. The latter will have to be (i) evaluated more microscopically, e.g., using input interactions from lQCD, and (ii) combined with radiative energy loss.

In the quarkonium sector, steady progress is made in implementing first-principle information from finite-T lattice QCD into effective models suitable for tests in heavy-ion reactions. T-matrix approaches incorporate effects of color-screening, parton-induced dissociation, and in-medium masses and widths of heavy quarks (which, in turn, connect to the open-flavor sector). We have suggested an sQGP signature in terms of stronger suppression for Υ relative to J/ψ, which would be a direct proof of J/ψ regeneration and carries large sensitivity to color screening of bottomonia.

Acknowledgments

This work was supported in part by a fellowship of the Spanish M. E. C., a Feodor-Lynen fellowship of the A.-v.-Humboldt foundation, and a U.S. National Science Foundation CAREER Award under grant PHY-0449489.

References

1. K. Adcox *et al.* [PHENIX Collaboration], *Nucl. Phys.* **A757**, 184 (2005).
2. J. Adams *et al.* [STAR Collaboration], *Nucl. Phys.* **A757**, 102 (2005).
3. M. Gyulassy, I. Vitev, X.N. Wang and B.W. Zhang, arXiv:nucl-th/0302077.

4. S.S. Adler *et al.* [PHENIX Collaboration], *Phys. Rev. Lett.* **96**, 032301 (2006).
5. B.I. Abelev *et al.* [STAR Collaboration], arXiv:nucl-ex/0607012.
6. H. van Hees and R. Rapp, *Phys. Rev. C* **71**, 034907 (2005).
7. G.D. Moore and D. Teaney, *Phys. Rev. C* **71**, 064904 (2005).
8. M.G. Mustafa, *Phys. Rev. D* **72**, 014905 (2005).
9. H. van Hees, V. Greco and R. Rapp, *Phys. Rev. C* **73**, 034913 (2006).
10. S. Wicks *et al.*, arXiv:nucl-th/0512076.
11. B. Svetitsky *Phys. Rev. D* **37**, 2484 (1988).
12. N. Armesto *et al.*, *Phys. Lett. B* **637**, 362 (2006).
13. D. Pal and M. G. Mustafa, *Phys. Rev. C* **60**, 034905 (1999).
14. V. Greco, R. Rapp and C. M. Ko *Phys. Lett. B* **595**, 202 (2004).
15. S.S. Adler *et al.* [PHENIX Collaboration], *Phys. Rev. C* **72**, 024901 (2005); S. Sakai, arXiv:nucl-ex/0510027.
16. W. Liu and C. M. Ko, arXiv:nucl-th/0603004.
17. R. Rapp, V. Greco and H. van Hees, arXiv:hep-ph/0510050.
18. J. Adams *et al.* [STAR Collaboration], *Phys. Rev. Lett.* **94**, 062301 (2005).
19. A.A.P. Suaide *et al.* [STAR Collaboration] *J. Phys. G* **30**, S1179 (2004).
20. V.A. Novikov *et al.*, *Phys. Rept.* **41**, 1 (1978).
21. N. Brambilla *et al.*, arXiv:hep-ph/0412158.
22. T. Matsui and H. Satz, *Phys. Lett. B* **178**, 416 (1986).
23. F. Karsch, M.T. Mehr and H. Satz, *Z. Phys. C* **37**, 617 (1988).
24. M. Asakawa and T. Hatsuda, *Phys. Rev. Lett.* **92**, 012001 (2004).
25. S. Datta *et al.*, *Phys. Rev. D* **69**, 094507 (2004).
26. E.V. Shuryak and I. Zahed, *Phys. Rev. C* **70**, 021901 (2004).
27. C.Y. Wong, *Phys. Rev. C* **72**, 034906 (2005).
28. W.M. Alberico *et al.*, *Phys. Rev. D* **72**, 114011 (2005).
29. A. Mocsy and P. Petreczky, *Phys. Rev. D* **73**, 074007 (2006).
30. M. Mannarelli and R. Rapp, *Phys. Rev. C* **72**, 064905 (2005).
31. C.Y. Wong, arXiv:hep-ph/0606200.
32. G. Röpke, D. Blaschke and H. Schulz, *Phys. Rev. D* **38**, 3589 (1988).
33. E.V. Shuryak, *Sov. J. Nucl. Phys.* **28**, 408 (1978); G. Bhanot and M. Peskin, *Nucl. Phys.* **B156**, 391 (1979).
34. L. Grandchamp and R. Rapp, *Phys. Lett. B* **523**, 60 (2001); *Nucl. Phys.* **A709**, 415 (2002).
35. L. Grandchamp *et al.*, *Phys. Rev. C* **73**, 064906 (2006).
36. F. Karsch and E. Laermann, arXiv:hep-lat/0305025.
37. R. Rapp, *Eur. Phys. J. A* **18**, 459 (2003).
38. D. Cabrera and R. Rapp, in preparation (2006).
39. L.S. Celenza, B. Huang and C.M. Shakin, *Phys. Rev. C* **59**, 1030 (1999).
40. L. Grandchamp *et al.*, *Phys. Rev. Lett.* **92**, 212301 (2004).
41. S.S. Adler *et al.* [PHENIX Collaboration], *Phys. Rev. Lett.* **94**, 082301 (2005).
42. P. Braun-Munzinger and J. Stachel, *Phys. Lett. B* **490**, 196 (2000).
43. L. Yan, P. Zhuang and N. Xu, arXiv:nucl-th/0608010.
44. H. Pereira Da Costa *et al.* [PHENIX Collaboration], arXiv:nucl-ex/0510051.
45. F. Karsch, D. Kharzeev and H. Satz, *Phys. Lett. B* **637**, 75 (2006).
46. X. Zhao and R. Rapp, work in progress (2006).